

IMDM containing 10% foetal bovine serum, penicillin 50 U/ml and streptomycin 50 µg/ml were incubated for 0, 5, 10, 15, and 20 min on ice and fixed. Repolymerisation experiments of fibroblasts were performed by incubating cells on ice for 20 min and then restoring them to 37 °C for 15 min. Cells were stained with a mouse monoclonal anti- α -tubulin antibody used at a dilution of 1:100. The secondary antibody was donkey anti-mouse IgG Alexa Fluor 488 used at a dilution of 1:1000.

Mitotic Index and mitotic spindle formation. Fibroblasts (passage 5) grown on glass coverslips were fixed with ice-cold methanol and stained with a mouse monoclonal anti- α -tubulin antibody and a rabbit polyclonal anti-phospho Histone H3 (pH3) (Ser10) antibody (MILLIPORE) at dilutions of 1:250 and 1:100, respectively. Secondary antibodies were donkey anti-mouse IgG Alexa Fluor 488 and donkey anti-rabbit IgG Alexa Fluor 594 (Life Technologies) at dilutions of 1:1000. The pH3 signal-positive mitotic fibroblasts were counted from at least 830 total cells.

In vitro scratch assay. The *in vitro* scratch assay was done as previously described³⁷. For each image, distances between one side of scratch and the other were measured using ImageJ and 50 readings of distances were measured for each sample.

Image acquisition. Slides were observed under a fluorescence microscope (Axio Imager M1; Carl Zeiss) equipped with a digital camera (AxioCam HRC; Carl Zeiss). COS7 cells and fibroblasts were observed at 630 \times and 400 \times magnifications, respectively. *In vitro* scratch assay, dishes were observed under Axiovert 200M (Carl Zeiss) equipped with a digital camera (AxioCam MRm; Carl Zeiss) and fibroblasts were observed at a 100 \times magnification. Images were captured with the same settings using AxioVision 4.8 software (Carl Zeiss).

Quantification of microtubule density and relative FLAG intensity. Quantification of microtubule density was performed as previously described²⁴. For each COS7 cell, a region of interest (ROI) was manually assigned along the edge of the cell by the free hand tool in ImageJ. We then calculated the area and the mean intensity of the ROI by using the ImageJ ROI manager. We used the KBI Line Extract plug-in for line extraction. The parameters were gwiSlter 5, mdnmsLen 20, pickup above 0.0, shaven Len 5, and del Len 5. The total length of the extracted lines was calculated by the KBI Line Feature plug-in in ImageJ for the α -tubulin staining and the FLAG staining. The total length of the extracted lines in a selected cell divided by the area of the cell gave the microtubule density. These plug-ins are available as part of the KBI ImageJ plug-in package (<http://hasezawa.ib.k.u-tokyo.ac.jp/zp/Kbi/ImageJKbiPlugins>). The relative FLAG intensity was determined in ImageJ by subtracting the mean red signal intensity of an untransfected cell from that of a transfected cell. The untransfected cell was in the same image as that of the transfected cell.

Statistical analysis. One-way ANOVA and Tukey's post-hoc analysis and a chi-square test were performed using IBM SPSS Statistics Version 22. Fisher's exact test and the Bonferroni correction were performed using R software. We considered $p < 0.05$ to be significant after correction.

References

- Barkovich, A. J., Guerrini, R., Kuzniecky, R. I., Jackson, G. D. & Dobyns, W. B. A developmental and genetic classification for malformations of cortical development: update 2012. *Brain* **135**, 1348–1369 (2012).
- Kerjan, G. & Gleeson, J. G. Genetic mechanisms underlying abnormal neuronal migration in classical lissencephaly. *Trends Genet* **23**, 623–630 (2007).
- Keays, D. A. *et al.* Mutations in alpha-tubulin cause abnormal neuronal migration in mice and lissencephaly in humans. *Cell* **128**, 45–57 (2007).
- Jaglin, X. H. *et al.* Mutations in the beta-tubulin gene TUBB2B result in asymmetrical polymicrogyria. *Nat Genet* **41**, 746–752 (2009).
- Poirier, K. *et al.* Mutations in the neuronal ss-tubulin subunit TUBB3 result in malformation of cortical development and neuronal migration defects. *Hum Mol Genet* **19**, 4462–4473 (2010).
- Tischfield, M. A. *et al.* Human TUBB3 mutations perturb microtubule dynamics, kinesin interactions, and axon guidance. *Cell* **140**, 74–87 (2010).
- Breuss, M. *et al.* Mutations in the beta-tubulin gene TUBB5 cause microcephaly with structural brain abnormalities. *Cell Rep* **2**, 1554–1562 (2012).
- Simons, C. *et al.* A *de novo* mutation in the beta-tubulin gene TUBB4A results in the leukoencephalopathy hypomyelination with atrophy of the basal ganglia and cerebellum. *Am J Hum Genet* **92**, 767–773 (2013).
- Cushion, T. D. *et al.* *De novo* mutations in the beta-tubulin gene TUBB2A cause simplified gyral patterning and infantile-onset epilepsy. *Am J Hum Genet* **94**, 634–641 (2014).
- Poirier, K. *et al.* Mutations in TUBG1, DYNC1H1, KIF5C and KIF2A cause malformations of cortical development and microcephaly. *Nat Genet* **45**, 639–647 (2013).
- Jaglin, X. H. & Chelly, J. Tubulin-related cortical dysgeneses: microtubule dysfunction underlying neuronal migration defects. *Trends Genet* **25**, 555–566 (2009).
- Miller, F. D. *et al.* Isoforms of alpha-tubulin are differentially regulated during neuronal maturation. *J Cell Biol.* **105**, 3065–3073 (1987).
- Tischfield, M. A., Cederquist, G. Y., Gupta, M. L., Jr. & Engle, E. C. Phenotypic spectrum of the tubulin-related disorders and functional implications of disease-causing mutations. *Curr Opin Genet Dev* **21**, 286–294 (2011).
- Jackson, A. P. Diversifying microtubules in brain development. *Nat Genet* **41**, 638–640 (2009).

15. Sui, H. & Downing, K. H. Structural basis of interprotofilament interaction and lateral deformation of microtubules. *Structure* **18**, 1022–1031 (2010).
16. Fry, A. E., Cushion, T. D. & Pilz, D. T. The genetics of lissencephaly. *Am J Med Genet C Semin Med Genet* **166C**, 198–210 (2014).
17. Jansen, A. C. *et al.* TUBA1A mutations: from isolated lissencephaly to familial polymicrogyria. *Neurology* **76**, 988–992 (2011).
18. Poirier, K. *et al.* Expanding the spectrum of TUBA1A-related cortical dysgenesis to Polymicrogyria. *Eur J Hum Genet* **21**, 381–385 (2013).
19. Zanni, G. *et al.* Description of a novel TUBA1A mutation in Arg-390 associated with asymmetrical polymicrogyria and mid-hindbrain dysgenesis. *Eur J Paediatr Neurol* **17**, 361–365 (2013).
20. Cushion, T. D. *et al.* Overlapping cortical malformations and mutations in TUBB2B and TUBA1A. *Brain* **136**, 536–548 (2013).
21. Fallet-Bianco, C. *et al.* Mutations in tubulin genes are frequent causes of various foetal malformations of cortical development including microlissencephaly. *Acta Neuropathol Commun* **2**, 69 (2014).
22. Bahi-Buisson, N. *et al.* Refinement of cortical dysgeneses spectrum associated with TUBA1A mutations. *J Med Genet* **45**, 647–653 (2008).
23. Kumar, R. A. *et al.* TUBA1A mutations cause wide spectrum lissencephaly (smooth brain) and suggest that multiple neuronal migration pathways converge on alpha tubulins. *Hum Mol Genet* **19**, 2817–2827 (2010).
24. Fujita, S. *et al.* An atypical tubulin kinase mediates stress-induced microtubule depolymerization in Arabidopsis. *Curr Biol* **23**, 1969–1978 (2013).
25. Bahi-Buisson, N. *et al.* The wide spectrum of tubulinopathies: what are the key features for the diagnosis? *Brain* **137**, 1676–1700 (2014).
26. Shimojima, K. *et al.* Whole-exome sequencing identifies a *de novo* TUBA1A mutation in a patient with sporadic malformations of cortical development: a case report. *BMC Res Notes* **7**, 465 (2014).
27. Tian, G. *et al.* Disease-associated mutations in TUBA1A result in a spectrum of defects in the tubulin folding and heterodimer assembly pathway. *Hum Mol Genet* **19**, 3599–3613 (2010).
28. Lowe, J., Li, H., Downing, K. H. & Nogales, E. Refined structure of alpha beta-tubulin at 3.5 Å resolution. *J Mol Biol* **313**, 1045–1057 (2001).
29. Brangwynne, C. P. *et al.* Microtubules can bear enhanced compressive loads in living cells because of lateral reinforcement. *J Cell Biol* **173**, 733–741 (2006).
30. Poirier, K. *et al.* Large spectrum of lissencephaly and pachygyria phenotypes resulting from *de novo* missense mutations in tubulin alpha 1A (TUBA1A). *Hum Mutat* **28**, 1055–1064 (2007).
31. Morris-Rosendahl, D. J. *et al.* Refining the phenotype of alpha-1a Tubulin (TUBA1A) mutation in patients with classical lissencephaly. *Clin Genet* **74**, 425–433 (2008).
32. Okumura, A. *et al.* Lissencephaly with marked ventricular dilation, agenesis of corpus callosum, and cerebellar hypoplasia caused by TUBA1A mutation. *Brain Dev* **35**, 274–279 (2013).
33. Okamoto, N. *et al.* KIF1A mutation in a patient with progressive neurodegeneration. *J. Hum. Genet.* **59**, 639–641 (2014).
34. Adzhubei, I. A. *et al.* A method and server for predicting damaging missense mutations. *Nat. Methods* **7**, 248–249 (2010).
35. Kumar, P. *et al.* Predicting the effects of coding non-synonymous variants on protein function using the SIFT algorithm. *Nat. Protoc.* **4**, 1073–1081 (2009).
36. Bradley, N. S. *et al.* Exome-wide rare variant analysis identifies TUBA4A mutations associated with familial ALS. *Neuron* **84**, 324–331 (2014).
37. Chun-achi, L. *et al.* *In vitro* scratch assay: a convenient and inexpensive method for analysis of cell migration *in vitro*. *Nat. Protoc.* **2**, 329–333 (2007).

Acknowledgments

This study was supported in part by a grant for Research on Applying Health Technology from the Ministry of Health, Labour and Welfare of Japan to F.M., N.O., M.K., M.Y., Y.K., K.K. and S.S.; by SENTAN, JST, Japan to I.Y. We thank the families and M. Hayakawa for their involvement and participation; H. Sui for the kind gift of the structural modelling data; and H. Inagaki, T. Ohye, T. Kato, and S. Yokoi for helpful discussions. We thank Mr. K. A. Boroevich for English proofreading.

Author Contributions

S.Y., M.T. and N.F. performed all experiments except whole-exome sequencing. F.M. performed whole-exome sequencing and the analysis. M.K., N.O., T.T., M.Y., Y.K., K.K. and S.S. participated in whole-exome sequencing. N.I., H.Y., S.K. and J.N. contributed materials. I.Y. constructed the microtubule structural model (Fig. 2). S.Y., N.I. and H.K. wrote the manuscript. All authors reviewed the manuscript.

Additional Information

Supplementary information accompanies this paper at <http://www.nature.com/srep>

Competing financial interests: The authors declare no competing financial interests.

How to cite this article: Yokoi, S. *et al.* TUBA1A mutation can cause a hydranencephaly-like severe form of cortical dysgenesis. *Sci. Rep.* **5**, 15165; doi: 10.1038/srep15165 (2015).



This work is licensed under a Creative Commons Attribution 4.0 International License. The images or other third party material in this article are included in the article's Creative Commons license, unless indicated otherwise in the credit line; if the material is not included under the Creative Commons license, users will need to obtain permission from the license holder to reproduce the material. To view a copy of this license, visit <http://creativecommons.org/licenses/by/4.0/>

Original article

Microarray analysis of 50 patients reveals the critical chromosomal regions responsible for 1p36 deletion syndrome-related complications

Shino Shimada^{a,b}, Keiko Shimojima^a, Nobuhiko Okamoto^c, Noriko Sangu^{a,d},
Kyoko Hirasawa^b, Mari Matsuo^e, Mayo Ikeuchi^f, Shuichi Shimakawa^g,
Kenji Shimizu^h, Seiji Mizunoⁱ, Masaya Kubota^j, Masao Adachi^k,
Yoshiaki Saito^l, Kiyotaka Tomiwa^m, Kazuhiro Haginoyaⁿ, Hironao Numabe^o,
Yuko Kako^p, Ai Hayashi^q, Haruko Sakamoto^r, Yoko Hiraki^s, Koichi Minami^t,
Kiyoshi Takemoto^u, Kyoko Watanabe^v, Kiyokuni Miura^w,
Tomohiro Chiyonobu^x, Tomohiro Kumada^y, Katsumi Imai^z,
Yoshihiro Maegaki^{aa}, Satoru Nagata^b, Kenjiro Kosaki^{ab},
Tatsuro Izumi^f, Toshiro Nagai^{ac}, Toshiyuki Yamamoto^{a,*}

^a Tokyo Women's Medical University Institute for Integrated Medical Sciences, Tokyo, Japan

^b Department of Pediatrics, Tokyo Women's Medical University, Tokyo, Japan

^c Department of Medical Genetics, Osaka Medical Center and Research Institute for Maternal and Child Health, Izumi, Japan

^d Department of Oral and Maxillofacial Surgery, School of Medicine, Tokyo Women's Medical University, Tokyo, Japan

^e Institute of Medical Genetics, Tokyo Women's Medical University, Tokyo, Japan

^f Department of Pediatrics and Child Neurology, Oita University Faculty of Medicine, Oita, Japan

^g Department of Pediatrics, Osaka Medical College, Takatsuki, Japan

^h Division of Medical Genetics, Saitama Children's Medical Center, Saitama, Japan

ⁱ Department of Pediatrics, Central Hospital, Aichi Human Service Center, Kasugai, Japan

^j Division of Neurology, National Center for Child Health and Development, Tokyo, Japan

^k Department of Pediatrics, Kakogawa Hospital Organization, Kakogawa West-City Hospital, Kakogawa, Japan

^l Department of Child Neurology, National Center of Neurology and Psychiatry, Tokyo, Japan

^m Department of Pediatrics, Medical Center for Children, Osaka City General Hospital, Osaka, Japan

ⁿ Department of Pediatric Neurology, Takuto Rehabilitation Center for Children, Sendai, Japan

^o Department of Genetic Counseling, Graduate School of Humanities and Sciences, Ochanomizu University, Tokyo, Japan

^p Department of Pediatrics, Showa University School of Medicine, Tokyo, Japan

^q Department of Neonatology, Japanese Red Cross Kyoto Daiichi Hospital, Kyoto, Japan

^r Department of Pediatrics, Osaka Red Cross Hospital, Osaka, Japan

^s Hiroshima Municipal Center for Child Health and Development, Hiroshima, Japan

^t Department of Pediatrics, Wakayama Medical University, Wakayama, Japan

^u Osaka Developmental Rehabilitation Center, Osaka, Japan

^v Department of Pediatrics, National Hospital Organization Kokura Medical Center, Kitakyushu, Japan

^w Developmental Disability Medicine, Nagoya University Graduate School of Medicine, Nagoya, Japan

^x Department of Pediatrics, Graduate School of Medical Science, Kyoto Prefectural University of Medicine, Kyoto, Japan

^y Department of Pediatrics, Shiga Medical Center for Children, Moriyama, Japan

^z National Epilepsy Center, Shizuoka Institute of Epilepsy and Neurological Disorders, Shizuoka, Japan

* Corresponding author. Address: Tokyo Women's Medical University Institute for Integrated Medical Sciences, 8-1 Kawada-cho, Shinjuku-ward, Tokyo 162-8666, Japan. Tel.: +81 3 3353 8111x24013; fax: +81 3 5269 7667.

E-mail address: yamamoto.toshiyuki@twmu.ac.jp (T. Yamamoto).

^{aa} Division of Child Neurology, Tottori University School of Medicine, Yonago, Japan

^{ab} Center for Medical Genetics, Keio University School of Medicine, Tokyo, Japan

^{ac} Department of Pediatrics, Dokkyo Medical University Koshigaya Hospital, Saitama, Japan

Received 2 April 2014; received in revised form 1 August 2014; accepted 5 August 2014

Abstract

Objective: Monosomy 1p36 syndrome is the most commonly observed subtelomeric deletion syndrome. Patients with this syndrome typically have common clinical features, such as intellectual disability, epilepsy, and characteristic craniofacial features.

Method: In cooperation with academic societies, we analyzed the genomic copy number aberrations using chromosomal microarray testing. Finally, the genotype–phenotype correlation among them was examined.

Results: We obtained clinical information of 86 patients who had been diagnosed with chromosomal deletions in the 1p36 region. Among them, blood samples were obtained from 50 patients (15 males and 35 females). The precise deletion regions were successfully genotyped. There were variable deletion patterns: pure terminal deletions in 38 patients (76%), including three cases of mosaicism; unbalanced translocations in seven (14%); and interstitial deletions in five (10%). Craniofacial/skeletal features, neurodevelopmental impairments, and cardiac anomalies were commonly observed in patients, with correlation to deletion sizes.

Conclusion: The genotype–phenotype correlation analysis narrowed the region responsible for distinctive craniofacial features and intellectual disability into 1.8–2.1 and 1.8–2.2 Mb region, respectively. Patients with deletions larger than 6.2 Mb showed no ambulation, indicating that severe neurodevelopmental prognosis may be modified by haploinsufficiencies of *KCNAB2* and *CHD5*, located at 6.2 Mb away from the telomere. Although the genotype–phenotype correlation for the cardiac abnormalities is unclear, *PRDM16*, *PRKCZ*, and *RERE* may be related to this complication. Our study also revealed that female patients who acquired ambulatory ability were likely to be at risk for obesity.

© 2014 The Japanese Society of Child Neurology. Published by Elsevier B.V. All rights reserved.

Keywords: 1p36 deletion syndrome; Chromosomal deletion; Genotype–phenotype correlation; Intellectual disability; Ambulation; Epilepsy; Distinctive features

1. Introduction

Monosomy 1p36 syndrome is a congenital malformation syndrome caused by the subtelomeric deletion of the short arm of chromosome 1 [1–3]. This syndrome is the most commonly observed subtelomere deletion syndrome, with an estimated incidence of 1:5000–1:10,000 [4,5]. Patients with this syndrome exhibit common clinical features, including intellectual disability (ID) and characteristic craniofacial features; such as straight eyebrows, deep-set eyes, epicanthus, and a pointed chin [6–9]. Although the levels of ID vary among patients, craniofacial features are commonly seen [10]. The patients with the 1p36 deletion syndrome also show many other complications, including hypotonia, seizures, hearing loss, structural heart defects, cardiomyopathy, ophthalmological abnormalities, and behavior abnormalities [7]. Recent advances in microarray-based chromosomal testing have helped us to identify small chromosomal rearrangements that are invisible by conventional G-banded chromosomal tests/karyotyping [11,12]. Using this method, the precise locations of the aberrations can be revealed at the molecular level. These advances have also allowed the study of more in-depth genotype–phenotype correlations for this syndrome, as

well as the identification of some of the regions responsible for individual complications [12,13].

In this study, we performed a nation-wide survey for the 1p36 deletion syndrome in Japan. The aim of this study was to identify the chromosomal regions responsible for individual complications in patients with 1p36 deletions. We analyzed the affected genomic regions in 50 patients with 1p36 deletions, and performed correlational analyses of the genotype data with the clinical information.

2. Materials and methods

2.1. Patients and samples

We performed a nation-wide survey for the 1p36 deletion syndrome with the cooperation of two academic societies; the Japanese Society of Child Neurology and the Japan Society of Pediatric Genetics. The study subjects were Japanese patients who had already been diagnosed using various diagnostic methods, including conventional karyotyping, subtelomere fluorescence *in situ* hybridization (FISH) analysis, multiplex ligation-dependent probe amplification (MLPA), and chromosomal microarray testing. Five patients

(patient [Pt] 8, 9, 21, 28, and 43), whose clinical features have been previously reported [14–17], were also included in this study. With the questionnaire survey for attending physicians, we accumulated the patients' clinical information, including craniofacial/skeletal features, neurodevelopmental features, brain structural abnormalities, cardiac abnormalities, sensory-organs abnormalities, urogenital abnormalities, endocrinological and nutritional findings among others. This study was approved by the ethics committee in Tokyo Women's Medical University.

On receipt of written informed consents from the families of the patients, we obtained the patients' blood samples to determine genomic copy number losses in the patients. Genomic DNA was extracted from the blood samples using the QIA quick DNA Extraction Kit (QIAGEN, Hamburg, Germany). Metaphase spreads were also prepared from blood samples and used for FISH analyses. In cases, if we could obtain written informed consent, parental samples were also analyzed.

2.2. Molecular and cytogenetic analyses

Chromosomal microarray testing was performed using any of the Agilent Oligo Microarray Kits 44, 60, 105, 180, and 244 K (Agilent Technologies, Santa Clara, CA), as described previously [18,19]. Genomic copy number aberrations were visualized using Agilent Genomic Workbench version 6.5 (Agilent Technologies). For cases in which variations of unknown significance were identified or suspected, parental samples were also analyzed. In cases of complex chromosomal rearrangements or mosaicism, metaphase spreads prepared using the patients' samples were used for FISH analyses for confirmation. The bacterial artificial clones were selected from the UCSC genome browser (<http://genome.ucsc.edu/>) for use as probes. For the target probes, RP11-425E15 (1p36.33: 949,400–1,132,489), RP11-82D16 (1p36.33: 2,046,751–2,208,312), RP11-70N12 (1p36.32: 2,740,703–2,922,551), CTD-3209F18 (1p36.32: 3,530,092–3,769,006), and RP11-933B18 (1p36.31: 5,988,719–6,177,261) were selected, while CTB-167K11 (1q44: 249,250,621–249,250,621) was used as a marker of chromosome 1. All of the genomic regions are described according to the February 2009 human reference sequence (GRCh37/hg19) in this study.

3. Results

3.1. Molecular-cytogenetic findings

We obtained clinical information from 86 patients with chromosomal deletions involving 1p36 regions. Among them, 50 patients (15 males and 35 females) were successfully genotyped. All of the genotypes were summarized in Tables 1 and 2, and 1p36 deletions identified

in the patients were depicted in the genome map (Fig. 2). The minimum and maximum deletion sizes was 0.9 and 12.9 Mb, respectively. Pure terminal deletions were identified in 38 patients (76%). Among them, three patients (Pt 8, 19, and 21) exhibited mosaicism. Pt 8 was first diagnosed with mosaic 1p36 deletion by chromosomal microarray testing, and Pt 21 had been diagnosed with 1p36 deletion using subtelomere FISH analysis; however, mosaicism was not reported at that time [17]. Although the mosaic deletion of 1p36 in Pt 19 had been firstly confirmed by FISH, we could not detect the breakpoint by chromosomal microarray testing due to low frequency (28% mosaic ratio). As the breakpoint was determined to be between two FISH probes (CTD-3209F18 and RP11-933B18), the proximal end of CTD-3209F18 was used as the minimum deletion region in this patient.

Additional aberrations with the sizes over 0.5 Mb were identified in eight patients (Pt 2, 10, 11, 15, 20, 28, 34, and 43) involving chromosomes 4, 7, 8, 13, and Y (Table 2), including a possible benign copy number aberration in Pt 15, which was also observed in the healthy mother. The other seven patients were confirmed to have unbalanced translocations by cytogenetic evaluation (14%), using either G-banding or FISH analysis. Two translocations were diagnosed as *de novo*, and the others were designated as unknown because of the lack of availability of parental information.

Five patients (Pt 1, 14, 47, 48, and 50) had interstitial deletions (10%) with a deletion size between 0.9 and 10.3 Mb.

3.2. Clinical findings

Clinical information of the 50 patients successfully genotyped is summarized in Table 3. Estimated frequencies of each complication are also included in Table 3. Pt 26 and 49 suddenly died at 24 and 10 months old of age, respectively. Pt 49 probably died due to heart failure but Pt 26 died of an unknown cause (detailed information unavailable).

3.2.1. Craniofacial features

Most of the patients showed craniofacial features, including straight eyebrows (84%), deep-set eyes (93%), broad nasal bridge (97%), low set ears (88%), and a pointed chin (89%). Constellations of these findings make distinctive facial impressions for 1p36 deletion syndrome, observed in Pt 3, 6, and 14 (Fig. 1b–d). This observation suggests that hypotelorism is rather characteristic among these patients. On the other hand, Pt 1 did not show deep-set eyes (Fig. 1a). The craniofacial features of three patients (Pt 47, 48, and 50) did not exhibit hypotelorism (Fig. 2e–g). From the genotypic point of view, these three patients (Pt 47, 48, and 50) would be diagnosed as having the proximal 1p36 deletion syndrome [20,21].

Table 1
The ranges of 1p36 deletions analyzed by chromosomal microarray testing.

Patient number	Age (year)	Gender	Platform (k)	Start ^a	End ^a	Additional aberration	FISH probe	Mosaic ratio ^b (%)	References
1	14	F	180	834,101	1,770,669	Interstitial	RP11-425E15		
2	9	M	44	1	1,820,584	der(1)t(Y;1), idic(Y)			
3	6	F	180	1	2,186,829				
4	1	F	60	1	2,239,497				
5	3	F	44	1	2,281,699				
6	5	F	60	1	2,553,982				
7	2	M	60	1	2,553,982				
8	5	F	44	1	3,044,953	Mosaicism	RP11-82D16	70	Shimada et al. [17]
9	13	F	44	1	3,102,718				Okamoto et al. [14]
10	18	F	44	1	3,102,718	der(1)t(1;7)			
11	17	F	60	1	3,138,565	der(1)t(1;8)			
12	8	F	60	1	3,265,702				
13	11	F	244	1	3,408,152				
14	5	M	60	1,786,789	3,472,907	Interstitial			
15	2	F	180	1	3,564,328				
16	13	M	60	1	3,582,084				
17	4	F	44	1	3,607,275				
18	2	F	60	1	3,660,110				
19	3	F	60	1	3,769,006	Mosaicism	CTD-3209F18	28	
20	3	M	44	1	4,070,842	der(1)t(1;13)			
21	17	F	44	1	4,481,324	Mosaicism	RP11-82D16	77	Shimada et al. [17]
22	2	F	180	1	4,703,581				
23	6	M	60	1	4,779,157				
24	3	F	60	1	4,843,370				
25	6	F	44	1	4,843,718				
26	2	M	60	1	5,252,985				
27	0	F	44	1	5,252,985				
28	25	F	44	1	5,411,803	der(1)t(Y;1)			Hiraki et al. [15]
29	3	F	44	1	6,128,223				
30	3	F	60	1	6,282,562				
31	1	F	60	1	6,282,562				
32	3	M	60	1	6,882,431				
33	7	M	60	1	7,035,075				
34	1	F	60	1	7,187,535	der(1)t(1;4)			
35	10	M	60	1	7,392,688				
36	8	M	60	1	7,581,058				
37	3	F	44	1	8,077,959				
38	2	F	60	1	8,104,671				
39	3	M	44	1	8,104,671				
40	4	M	44	1	8,181,042				
41	5	F	44	1	8,181,042				
42	1	F	60	1	8,427,633				
43	3	M	60	1	9,180,975	der(1)(1;4)			Saito et al. [16]
44	5	F	60	1	9,251,936				
45	4	M	60	1	9,953,030				

46	2	F	44	1	10,001,011	Interstitial
47	4	F	44	2,080,309	10,869,155	Interstitial
48	8	F	60	2,785,042	12,743,178	Interstitial
49	0	F	44	1	12,917,483	Interstitial
50	22	F	180	6,614,950	16,890,814	Interstitial

^a The genomic position referring build19.

^b The mosaic ratio was confirmed by FISH; F, female; M, male.

3.2.2. Neurological features

Almost all patients showed ID (98%) but a patient (Pt 2) having a deletion in the far distal region of 1p36 showed borderline ID, with an intelligence quotient (IQ) of 80. Therefore, this region could be eliminated from the responsible region for ID (Fig. 2). The smallest deletion, an interstitial deletion between genomic positions 0.8 and 1.8 Mb, was identified in Pt 1 (Fig. 2). In spite of having this smallest deletion, Pt 1 had severe ID, i.e., she was locomotive but aphasic and required support for all activities in her daily life. This was probably a consequence of intractable epilepsy associated with tonic seizures, caused by factors other than the interstitial deletion of this region. The proximal and distal ends of the breakpoints in Pt 3 and 14 defined the shortest region of overlap for ID, spanning the 1.8–2.2 Mb region (Fig. 2; region B). Axial hypotonia (92%) and poor sucking (70%) were also commonly observed. Epilepsy, one of the major complications in 1p36 deletion syndrome, was observed in 70% of the patients. Infantile spasms were observed in 16% of the patients.

In this study, many types of structural brain abnormalities were identified; not only in the cerebral cortex but also in the white matter (Table 3), indicating that there is no major pattern. The most frequently observed abnormality was a nonspecific finding with enlargement of lateral ventricles.

3.2.3. Cardiac abnormality

Cardiac abnormality is one of the most frequently observed complications in patients with 1p36 deletions. In this study, congenital heart defects and functional abnormalities were observed in 69% (34/49) and 22% (11/49) of the patients, respectively. The most frequently observed patterns were patent ductus arteriosus (PDA; 37% [18/49]) and ventricular septal defects (VSD; 37% [18/49]).

3.2.4. Other complications

Many kinds of complications were observed in many organs. Cryptorchidism was the most frequently observed complication in male patients (64% [9/14]). As Pt 14, with a small interstitial deletion spanning from 1.8 to 3.5 Mb, had cryptorchidism, the deleted region was likely involved in abnormalities of the external genitalia (Fig. 2; region H). Hearing problems (39% [19/49]) and strabismus (33% [15/46]) were relatively common among the patients. Obesity was observed in 5 patients (11% [5/46]).

Renal abnormalities were rare and identified only in three patients. Among them, Pt 26, who had a 5.3 Mb deletion, was diagnosed with the autosomal recessive cystic kidney disease of nephronophthisis (this patient died at 2 years of age) [22]. One of the genes responsible for this condition, the nephronophthisis 4 gene

Table 2
Additional aberrations identified in the patients.

Patient number	Chr	Start ^a	End ^a	Remark	Attribute	Origin
2	Y	1	59,373,566	der(1)t(Y;1)(p36.3;q12), idic(Y)(q12)	dup	NA
10	7	1	6,870,943	der(1)t(1;7)(p36.32;p22.1)	dup	NA
11	8	1	3,909,039	der(1)t(1;8)(p36.22;p23.2)	dup	NA
15	1	146,324,068	149,192,104	del(1)(q21.1;q21.2)	del	Common with mother
20	13	100,462,233	115,169,878	der(1)t(1;13)(p26.32;q32.3)	dup	De novo
28	Y	26,435,039	59,373,566	der(1)t(Y;1)(q12;p36.32) [#]	dup	NA
34	4	1	13,396,747	der(1)t(1;4)(p36.31;p15.33)	dup	De novo
43	4	189,012,426	191,154,276	der(1)t(1;4)(p36.31;q35.2)	dup	NA

^a The genomic position referring build19; dup, duplication; del, deletion; NA, not available.

[#] This case was previously reported by Hiraki et al. [15].

(*NPHP4*), is located on 1p36 (chr1: 5,946,555–5,965,543) [23], proximal to the deletion region of three patients with renal abnormalities (Pt 26, 33, and 35). It is unclear whether there is a correlation between *NPHP4* and the renal abnormalities observed in this study.

4. Discussion

4.1. Previous genetic studies on the 1p36 deletion syndrome

Many cohort studies have been performed to delineate the phenotypic features of patients with 1p36 deletion syndrome and to evaluate the frequency of complications [1,6,7]. It has been reported that there is no correlation between the deletion size and the number of observed clinical features [24], while the critical region responsible for core phenotypic features, including clefting, hypothyroidism, cardiomyopathy, hearing loss, large fontanel, and hypotonia, has been narrowed down to a region 2.2 Mb from the telomere [3]. Compared to such core phenotypic features, other complications tend to vary with the size of the deletion, and study subjects with larger deletions tend to have more phenotypic features [25], suggesting that the various phenotypic features are dependent on genes involved in the deletion regions. Thus, precise knowledge of the genotype–phenotype correlations could potentially lead to more personalized treatments for individuals with 1p36 deletions and might identify mutations for single gene disorders [3]. The potassium voltage-gated channel, shaker-related subfamily, beta member 2 gene (*KCNAB2*) and the v-ski sarcoma viral oncogene homolog gene (*SKI*) were identified as candidate genes for the epilepsy phenotype and clefting abnormalities, respectively [26,27]. More recently, the PR domain containing 16 gene (*PRDM16*) was identified as a possible candidate gene for cardiomyopathy, as *PRDM16* was included in a minimal deletion among patients with 1p36 deletions associated with cardiomyopathy, while in patients with pure cardiomyopathy, single nucleotide variants

of *PRDM16* were identified as the cause of cardiomyopathy [28]. This was one of the most successful studies of genotype–phenotype correlation in patients with 1p36 deletions [28].

4.2. Craniofacial features

As mentioned above, a region 2.2 Mb from the telomere has been reported to be responsible for core phenotypic features of 1p36 deletion syndrome [3]. Compared to this, we observed atypical facial features in four patients (Pt 1, 47, 48, and 50) whose deletions did not include the 1.8–2.1 Mb region, in this study. Thus, the region responsible for typical facial features is narrowed into this region (Fig. 2; region A). Because hypotelorism has never been listed in the clinical delineations of 1p36 deletion syndrome reported from Western countries, we did not include this finding in the questionnaire survey and the frequency of this finding in Japanese patients could not be calculated. However, it is commonly observed in Japanese patients with typical 1p36 deletion syndrome. Therefore, hypotelorism may be a characteristic finding among Asian patients.

4.3. Neurological features

Although more severe ID was reported to be associated with larger 1p36 deletions [10], the genomic region responsible for severe ID has never been identified. In this study, a patient (Pt 28) having a 5.4 Mb deletion acquired independent gait, while patients with >6.1 Mb deletions had not yet acquired independent gait, and exhibited severe ID. Thus, the region between 5.4 and 6.1 Mb would appear to be the borderline for independent gait (Fig. 2; region C), and the modifier genes for prognosis of development may be located in the region proximal to this borderline. *KCNAB2*, mentioned above, may be one of the modifier genes responsible for severe ID. Chromodomain helicase DNA-binding protein 5 (*CHD5*; chr1: 6,161,847–6,240,194), which encodes a neuron-specific protein, is

Table 3

Summary of clinical features of the patients with 1p36 deletions.

Patient number	1	2	3	4	5	6	7	8	9	10	11	12	13	14	15	16	17	18	19	20	21	22	23	24	25	26	27	28	29	30	31	32	33	34	35	36	37	38	39	40	41	42	43	44	45	46	47	48	49	50	Frequencies		
1. Craniofacial and skeletal features																																																					
Characteristic craniofacial features																																																					
Microcephaly	NA	+	NA	+	+	NA	NA	-	+	NA	+	NA	NA	+	NA	NA	NA	+	NA	83% (20/24)																																	
Brachycephaly	+	NA	-	+	+	NA	NA	-	+	NA	+	NA	NA	-	NA	NA	NA	+	NA	NA	65% (11/17)																																
Straight eyebrow	-	+	+	+	+	+	+	+	+	+	+	+	+	+	+	+	+	+	+	+	+	+	+	+	+	+	+	+	+	+	+	+	+	+	+	+	+	+	+	+	+	+	+	+	+	+	+	+	+	+	84% (32/38)		
Deep-set eyes	-	+	+	+	+	+	+	+	+	+	+	+	+	+	+	+	+	+	+	+	+	+	+	+	+	+	+	+	+	+	+	+	+	+	+	+	+	+	+	+	+	+	+	+	+	+	+	+	+	+	93% (37/40)		
Epicanthus	+	NA	+	+	+	+	+	+	+	+	+	+	+	+	+	+	+	+	+	+	+	+	+	+	+	+	+	+	+	+	+	+	+	+	+	+	+	+	+	+	+	+	+	+	+	+	+	+	+	86% (30/35)			
Broad nasal root/bridge	+	NA	+	+	+	+	+	+	+	+	+	+	+	+	+	+	+	+	+	+	+	+	+	+	+	+	+	+	+	+	+	+	+	+	+	+	+	+	+	+	+	+	+	+	+	+	+	+	+	97% (32/33)			
Long philtrum	+	+	+	+	+	+	+	+	+	+	+	+	+	+	+	+	+	+	+	+	+	+	+	+	+	+	+	+	+	+	+	+	+	+	+	+	+	+	+	+	+	+	+	+	+	+	+	+	+	63% (22/35)			
Low set ears	-	+	+	+	+	+	+	+	+	+	+	+	+	+	+	+	+	+	+	+	+	+	+	+	+	+	+	+	+	+	+	+	+	+	+	+	+	+	+	+	+	+	+	+	+	+	+	+	+	88% (29/33)			
Pointed chin	+	+	+	+	+	+	+	+	+	+	+	+	+	+	+	+	+	+	+	+	+	+	+	+	+	+	+	+	+	+	+	+	+	+	+	+	+	+	+	+	+	+	+	+	+	+	+	+	+	+	89% (34/38)		
Late closure of the anterior fontanel	-	NA	+	-	-	NA	NA	+	+	NA	NA	NA	NA	+	NA	NA	NA	+	+	+	+	+	+	+	+	+	+	+	+	+	+	+	+	+	+	+	+	+	+	+	+	+	+	+	+	+	+	+	+	56% (18/32)			
Cleft palate problem																																																					
High palate	-	-	-	-	-	-	-	+	-	+	-	-	-	-	-	-	-	-	-	-	-	-	-	-	-	-	-	-	-	-	-	-	-	-	-	-	-	-	-	-	-	-	-	-	-	-	-	-	-	-	29% (14/49)		
Cleft palate	-	-	+	-	-	-	-	-	-	-	-	+	-	+	-	-	-	-	-	-	-	-	-	-	-	-	-	-	-	-	-	-	-	-	-	-	-	-	-	-	-	-	-	-	-	-	-	-	-	-	22% (11/49)		
Cleft lip	-	-	-	-	-	-	-	-	-	-	-	-	-	-	-	-	-	-	-	-	-	-	-	-	-	-	-	-	-	-	-	-	-	-	-	-	-	-	-	-	-	-	-	-	-	-	-	-	-	-	16% (8/49)		
Cleft jaw	-	-	-	-	-	-	-	-	-	-	-	-	-	-	-	-	-	-	-	-	-	-	-	-	-	-	-	-	-	-	-	-	-	-	-	-	-	-	-	-	-	-	-	-	-	-	-	-	-	-	2% (1/50)		
Limb abnormalities																																																					
Finger abnormalities	-	-	NA	-	-	-	-	-	-	-	-	NA	-	+	-	+	-	+	-	-	-	-	-	-	-	-	-	-	-	-	-	-	-	-	-	-	-	-	-	-	-	-	-	-	-	-	-	-	-	-	-	15% (7/48)	
Limb deformity	-	-	NA	-	-	-	-	-	-	-	-	NA	-	-	-	-	-	-	-	-	-	-	-	-	-	-	-	-	-	-	-	-	-	-	-	-	-	-	-	-	-	-	-	-	-	-	-	-	-	-	4% (2/48)		
Other skeletal abnormalities																																																					
Rib abnormalities such as 11 ribs	-	-	NA	-	-	-	-	-	-	-	-	NA	-	-	-	-	-	-	-	-	-	-	-	-	-	-	-	-	-	-	-	-	-	-	-	-	-	-	-	-	-	-	-	-	-	-	-	-	-	-	4% (2/48)		
Scoliosis	-	-	NA	-	-	-	-	-	-	-	-	NA	-	-	-	-	-	-	-	-	-	-	-	-	-	-	-	-	-	-	-	-	-	-	-	-	-	-	-	-	-	-	-	-	-	-	-	-	-	-	25% (12/48)		
Congenital dislocated hip	-	-	NA	-	-	-	-	-	-	-	-	NA	-	-	-	-	-	-	-	-	-	-	-	-	-	-	-	-	-	-	-	-	-	-	-	-	-	-	-	-	-	-	-	-	-	-	-	-	-	-	4% (2/48)		
Developmental dysplasia of the hip	-	-	NA	-	-	-	-	-	-	-	-	NA	-	-	-	-	-	-	-	-	-	-	-	-	-	-	-	-	-	-	-	-	-	-	-	-	-	-	-	-	-	-	-	-	-	-	-	-	-	-	2% (1/48)		
2. Neurological features (clinical)																																																					
Axial hypotonia	+	+	NA	-	+	+	+	+	+	+	+	+	+	+	+	+	+	+	+	+	+	+	+	+	+	+	+	+	+	+	+	+	+	+	+	+	+	+	+	+	+	+	+	+	+	+	+	+	+	+	+	92% (44/48)	
Poor sucking	-	-	NA	-	-	-	-	-	-	-	-	+	+	+	+	+	+	+	+	+	+	+	+	+	+	+	+	+	+	+	+	+	+	+	+	+	+	+	+	+	+	+	+	+	+	+	+	+	+	+	+	+	70% (32/46)
Difficulty of swallowing	-	-	+	-	-	-	-	-	-	-	-	+	+	+	+	+	+	+	+	+	+	+	+	+	+	+	+	+	+	+	+	+	+	+	+	+	+	+	+	+	+	+	+	+	+	+	+	+	+	+	+	+	56% (27/48)
Developmental delay																																																					
Intellectual disability	S	B	S	S	M	S	S	M	S	S	S	S	S	M	S	S	M	S	S	S	M	S	M	M	S	S	NA	S	M	S	S	S	S	S	S	S	S	S	S	S	S	S	S	S	S	S	S	S	S	S	S	98% (49/50)	
Acquire independent gait	+	+	+	-	+	+	+	+	+	+	+	+	+	+	+	+	+	+	+	+	+	+	+	+	+	+	+	+	+	+	+	+	+	+	+	+	+	+	+	+	+	+	+	+	+	+	+	+	+	+	+	32% (16/50)	
Expressive language																																																					
Sentence	-	+	-	-	-	-	-	-	-	-	-	+	-	-	-	-	-	-	-	-	-	-	-	-	-	-	-	-	-	-	-	-	-	-	-	-	-	-	-	-	-	-	-	-	-	-	-	-	-	-	-	6% (3/50)	
Only words	-	-	-	+	+	+	+	+	+	+	+	+	+	+	+	+	+	+	+	+	+	+	+	+	+	+	+	+	+	+	+	+	+	+	+	+	+	+	+	+	+	+	+	+	+	+	+	+	+	+	+	+	16% (8/50)
Dysarthria	-	+	-	-	-	-	-	-	-	-	-	+	-	-	-	-	-	-	-	-	-	-	-	-	-	-	-	-	-	-	-	-	-	-	-	-	-	-	-	-	-	-	-	-	-	-	-	-	-	-	-	8% (4/50)	
Gestures	-	-	-	-	-	-	-	-	-	-	-	+	-	-	-	-	-	-	-	-	-	-	-	-	-	-	-	-	-	-	-	-	-	-	-	-	-	-	-	-	-	-	-	-	-	-	-	-	-	-	-	10% (5/50)	
Behavior disorders																																																					
Self-injury	-	+	+	-	-	NA	+	-	NA	+	+	NA	+	NA	-	NA	-	NA	+	-	-	NA	-	NA	-	NA	+	+	+	-	-	-	-	-	-	-	-	-	-	-	-	-	-	-	-	-	-	-	-	-	-	30% (11/37)	
Temper tantrum	+	-	-	-	-	NA	+	+	NA	+	+	NA	+	NA	-	NA	-	NA	+	-	-	NA	+	NA	-	NA	+	+	-	-	-	-	-	-	-	-	-	-	-	-	-	-	-	-	-	-	-	-	-	-	-	30% (11/37)	
Poor social interaction	+	-	+	+	-	NA	+	+	NA	+	+	NA	+	NA	-	NA	-	NA	+	-	-	NA	-	NA	-	NA	+	-	-	-	-	-	-	-	-	-	-	-	-	-	-	-	-	-	-	-	-	-	-	-	-	27% (10/37)	
Epilepsy																																																					
History of epilepsy	+	-	+	+	-	+	-	+	+	+	+	+	+	+	+	+	+	+	+	+	+	+	+	+	+	+	+	+	+	+	+	+	+	+	+	+	+	+	+	+	+	+	+	+	+	+	+	+	+	+	+	+	70% (35/50)
Infantile spasms	-	-	-	+	-	-	+	-	-	-	-	-	-	-	-	-	-	-	-	-	-	-	-	-	-	-	-	-	-	-	-	-	-	-	-	-	-	-	-	-	-	-	-	-	-	-	-	-	-	-	-	16% (8/50)	
3. Neurological features (radiological)																																																					
Cerebral cortex																																																					
Periventricular nodular heterotopia (PVNH)	-	-	NA	-	-	-																																															



Fig. 1. Facial features of the patients with variably sized 1p36 deletions. Pt 1 (a; at 14 years of age) shows edematous eyelids rather than deep-set eyes. Pt 3 (b; 6 years), 6 (c; 5 years), and 14 (d; 15 years) share characteristic features, including deep-set eyes, hypotelorism, and pointed chins. Pt 47 (e; 4 years) and 48 (f; 8 years) do not exhibit such characteristic features, with round faces rather than hypotelorism and pointed chins. Pt 50 (g; 3 years) exhibits distinctive features with arched eyebrows and hypertelorism. Written informed consent to publish patient photos was obtained from all the patient families.

involved in chromatin remodeling and gene transcription, regulating the expression of neuronal genes [29]. Thus, *CHD5* also may be a modifier gene for severe ID.

It has been suggested that two genes, gamma-aminobutyric acid (GABA) A receptor delta (*GABRD*; chr1: 1,950,768–1,962,192), and *KCNAB2* (chr1: 6,105,981–6,161,253), are associated with the manifestations of epilepsy [27]. This is also been suggested by our present study, as there was no history of epilepsy in a patient (Pt 2) with a 1.8 Mb terminal deletion and a patient (Pt 50) with a 10.0 Mb interstitial deletion; both of the deletions includes neither *GABRD* nor *KCNAB2* (Fig. 2). The incidence of epilepsy was higher in the patients with severe ID (30/38; 79%) than in the patients with moderate ID (4/8; 50%). Thus, the severity of ID was associated with the incidence of epilepsy and the same gene/set of genes may be involved in both of these neurological manifestations.

Several case reports have suggested an association between periventricular nodular heterotopia (PVNH) and 1p36 deletion [16,30–32], and the candidate region for polymicrogyria has been mapped to the distal 4.8 Mb region [33]. As the smallest deletion among the patients with abnormal neuronal migration was 3.0 Mb (Pt 8), the gene(s) responsible for this phenotype may be narrowed down to the distal 3.0 Mb region (Fig. 2; region D). Chiari malformation type II was identified only in Pt 34, who showed an unbalanced translocation with chromosome 4. Thus, this rare feature may be attributable to the partial trisomy of chromosome 4.

4.4. Cardiac abnormality

Previously, the genetic region responsible for left ventricular noncompaction (LVNC) was assigned to the 1.9–3.4 Mb region [34–36]. On the other hand, there are many reports which show an association between Ebstein anomaly and 1p36 deletion [7,37–40]. The genomic region responsible for Ebstein anomaly was assigned to the 2.9–3.8 Mb region [39,40]. In 2005, Sinkovec et al. reported two patients with LVNC associated with Ebstein anomaly [41]. In this study, we identified a patient (Pt 24) who showed both LVNC and Ebstein anomalies. Given this perspective, it might be reasonable to conclude that the critical regions involved in LVNC and Ebstein anomaly are relatively close. As mentioned above *PRDM16* located on chr1: 2,985,742–3,355,185 was reported as a gene responsible for cardiomyopathy and LVNC [28]. This is in agreement with our study, as the smallest deletion identified in a patient (Pt 9) with DCM was 3.1 Mb in size. It is possible that *PRDM16* may also be related not only to LVNC but also to the Ebstein anomaly.

Although double-outlet right ventricle (DORV) has never been reported in individuals with 1p36 deletions, we found DORV in two patients. We found a relatively small deletion (2.5 Mb) in a patient (Pt 6) with DORV (Fig. 2; region D). There is a possibility that the protein kinase C zeta gene (*PRKCZ*; chr1: 1,981,909–2,116,834) is related to cardiac abnormalities, because this gene had been implicated in a variety of process including cardiac muscle function [42,43]. The positional

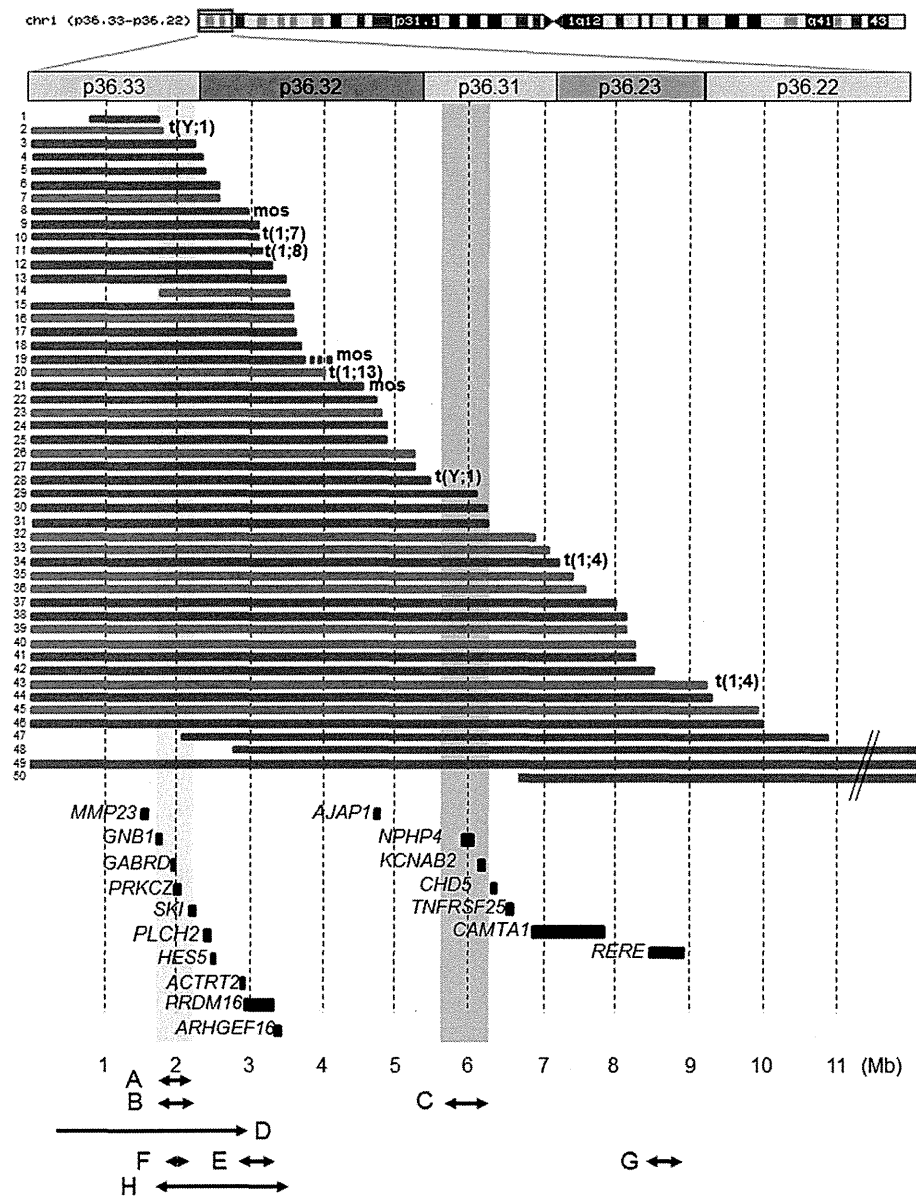


Fig. 2. Result of chromosomal microarray testing depicted in a genome map of the 1p36 region. The scheme of chromosome 1 (top) is downloaded from the UCSC genome browser. Red and blue bars indicate the deletion regions identified in female and male patients, respectively. Black bars indicate the locations of the genes, discussed in the text. The numbers depicted on the left side of each bar indicate patients' numbering. "t" and "mos" indicate unbalanced translocations and mosaicism, respectively. Yellow and green translucent vertical lines emphasize the proposed responsible regions for ID. Proposed responsible regions for each phenotype; A, distinctive craniofacial findings; B, ID; C, modifier effect for ID; D, LVNC and Ebstein anomaly; E, DORV; F, cardiac anomalies; G, cryptochidisms. (For interpretation of the references to color in this figure legend, the reader is referred to the web version of this article.)

effects for *PRDM16* may be another possibility in this case.

The arginine-glutamic acid dipeptide (RE) repeats gene (*RERE*; chr1: 8,412,464–8,877,699) has been reported to play a critical role in early cardiovascular development [44]. In this study, all patients with deletions larger than 8.4 Mb, which involve *RERE*, showed cardiac anomalies. Thus, *RERE* may be involved in the pathogenesis of congenital heart defects (Fig. 2; region G).

Only Pt 20, with an unbalanced translocation between 13q32.3, showed hypoplasia of the left ventricle (HLHS) in this study. HLHS accounts for 2–3% of all congenital heart defects, and a minority of HLHS cases have been associated with congenital anomaly syndromes, e.g., the Jacobsen, Turner, and Potocki–Lupski syndromes, respectively [45–47]. As 13q duplication has been reported to be associated with this manifestation, the findings of HLHS found in Pt 20 may be due to a partial trisomy of 13q [48].

4.5. Other complications

In patients with 1p36 monosomy, a Prader–Willi syndrome (PWS)-like phenotype has been described [6,13,49]. The clinical features that overlap between the 1p36 deletion syndrome and PWS are ID, neonatal hypotonia, obesity, craniofacial anomalies, hyperphagia, short stature, and behavior problems. D'Angelo et al. described a patient with a 2.5 Mb deletion within the chromosome region 1p36.33–1p36.32 [13]. Tsuyusaki et al. hypothesized that the critical region for the PWS-like phenotype was within 4 Mb from 1pter [49]. Rosenfeld et al. suggested a critical region for the PWS-like phenotype in the 1.7–2.3 Mb region [12]. In this study, all five patients with obesity (Pt 8, 10, 11, 13, and 21) were female, and acquired ambulatory ability within the ages of 2–8 years. Two of the patients (Pt 8 and 21) showed mosaic deletions [17]. From these perspectives, we speculate that female patients who showed 1p36 deletions involving the critical region and who acquired ambulatory ability are likely to be at risk for obesity.

5. Conclusion

In this study, we successfully accumulated the genotype–phenotype data of 50 patients with the deletions of 1p36 regions. As hypotelorism was commonly observed in patients, it may be characteristic of Asian patients. The genotype–phenotype correlation analysis narrowed down the regions responsible for distinctive craniofacial features and ID to the 1.8–2.1 and 1.8–2.2 Mb regions, respectively. Patients with deletions larger than 6.2 Mb showed no ambulation, indicating that severe neurodevelopmental prognosis may be modified by haploinsufficiencies of *KCNAB2* and/or *CHD5*, located 6.2 Mb away from the telomere. Although the genotype–phenotype correlation for the cardiac abnormalities is unclear, *PRDM16*, *PRKCZ*, and *RERE* may be related to this complication. One more finding revealed by this study for the first time, is that female patients who acquired ambulatory ability are likely to be at a risk for obesity.

Acknowledgments

We would like to express our gratitude to the patients and their families for their cooperation. We also thank the Japanese Society of Child Neurology and the Japan Society of Pediatric Genetics for their supports. This work was supported by a Grant-in-Aid for Scientific Research from Health Labor Sciences Research Grants from the Ministry of Health, Labor, and Welfare, Japan.

References

- [1] Shapira SK, McCaskill C, Northrup H, Spikes AS, Elder FFB, Sutton VR, et al. Chromosome 1p36 deletions: the clinical phenotype and molecular characterization of a common newly delineated syndrome. *Am J Hum Genet* 1997;61:642–50.
- [2] Gajecka M, Yu W, Ballif BC, Glotzbach CD, Bailey KA, Shaw CA, et al. Delineation of mechanisms and regions of dosage imbalance in complex rearrangements of 1p36 leads to a putative gene for regulation of cranial suture closure. *Eur J Hum Genet* 2005;13:139–49.
- [3] Heilstedt HA, Ballif BC, Howard LA, Lewis RA, Stal S, Kashork CD, et al. Physical map of 1p36, placement of breakpoints in monosomy 1p36, and clinical characterization of the syndrome. *Am J Hum Genet* 2003;72:1200–12.
- [4] Shao L, Shaw CA, Lu XY, Sahoo T, Bacino CA, Lalani SR, et al. Identification of chromosome abnormalities in subtelomeric regions by microarray analysis: a study of 5,380 cases. *Am J Med Genet A* 2008;146A:2242–51.
- [5] Heilstedt HA, Ballif BC, Howard LA, Kashork CD, Shaffer LG. Population data suggest that deletions of 1p36 are a relatively common chromosome abnormality. *Clin Genet* 2003;64:310–6.
- [6] Slavotinek A, Shaffer LG, Shapira SK. Monosomy 1p36. *J Med Genet* 1999;36:657–63.
- [7] Battaglia A, Hoyne HE, Dallapiccola B, Zackai E, Hudgins L, McDonald-McGinn D, et al. Further delineation of deletion 1p36 syndrome in 60 patients: a recognizable phenotype and common cause of developmental delay and mental retardation. *Pediatrics* 2008;121:404–10.
- [8] Battaglia A. Del 1p36 syndrome: a newly emerging clinical entity. *Brain Dev* 2005;27:358–61.
- [9] Zenker M, Rittinger O, Grosse KP, Speicher MR, Kraus J, Rauch A, et al. Monosomy 1p36—a recently delineated, clinically recognizable syndrome. *Clin Dysmorphol* 2002;11:43–8.
- [10] Kurosawa K, Kawame H, Okamoto N, Ochiai Y, Akatsuka A, Kobayashi M, et al. Epilepsy and neurological findings in 11 individuals with 1p36 deletion syndrome. *Brain Dev* 2005;27:378–82.
- [11] Buck A, du Souich C, Boerkoel CF. Minimal genotype–phenotype correlation for small deletions within distal 1p36. *Am J Med Genet A* 2011;155A:3164–9.
- [12] Rosenfeld JA, Crolla JA, Tomkins S, Bader P, Morrow B, Gorski J, et al. Refinement of causative genes in monosomy 1p36 through clinical and molecular cytogenetic characterization of small interstitial deletions. *Am J Med Genet A* 2010;152A:1951–9.
- [13] D'Angelo CS, Da Paz JA, Kim CA, Bertola DR, Castro CIE, Varela MC, et al. Prader–Willi-like phenotype: investigation of 1p36 deletion in 41 patients with delayed psychomotor development, hypotonia, obesity and/or hyperphagia, learning disabilities and behavioral problems. *Eur J Med Genet* 2006;49:451–60.
- [14] Okamoto N, Toribe Y, Nakajima T, Okinaga T, Kurosawa K, Nonaka I, et al. A girl with 1p36 deletion syndrome and congenital fiber type disproportion myopathy. *J Hum Genet* 2002;47:556–9.
- [15] Hiraki Y, Fujita H, Yamamori S, Ohashi H, Eguchi M, Harada N, et al. Mild craniosynostosis with 1p36.3 trisomy and 1p36.3 deletion syndrome caused by familial translocation t(Y;1). *Am J Med Genet A* 2006;140A:1773–7.
- [16] Saito Y, Kubota M, Kurosawa K, Ichihashi I, Kaneko Y, Hattori A, et al. Polymicrogyria and infantile spasms in a patient with 1p36 deletion syndrome. *Brain Dev* 2011;33:437–41.
- [17] Shimada S, Maegaki Y, Osawa M, Yamamoto T. Mild developmental delay and obesity in two patients with mosaic 1p36 deletion syndrome. *Am J Med Genet A* 2014;164A:415–20.
- [18] Shimada S, Okamoto N, Hirasawa K, Yoshii K, Tani Y, Sugawara M, et al. Clinical manifestations of Xq28 functional

- disomy involving MECP2 in one female and two male patients. *Am J Med Genet A* 2013;161A:1779–85.
- [19] Shimada S, Okamoto N, Ito M, Arai Y, Momosaki K, Togawa M, et al. MECP2 duplication syndrome in both genders. *Brain Dev* 2013;35:411–9.
- [20] Kang SH, Scheffer A, Ou Z, Li J, Scaglia F, Belmont J, et al. Identification of proximal 1p36 deletions using array-CGH: a possible new syndrome. *Clin Genet* 2007;72:329–38.
- [21] Shimojima K, Paez MT, Kurosawa K, Yamamoto T. Proximal interstitial 1p36 deletion syndrome: the most proximal 3.5-Mb microdeletion identified on a dysmorphic and mentally retarded patient with inv(3)(p14.1q26.2). *Brain Dev* 2009;31:629–33.
- [22] Benzing T, Schermer B. Clinical spectrum and pathogenesis of nephronophthisis. *Curr Opin Nephrol Hypertens* 2012;21:272–8.
- [23] Otto EA, Ramaswami G, Janssen S, Chaki M, Allen SJ, Zhou W, et al. Mutation analysis of 18 nephronophthisis associated ciliopathy disease genes using a DNA pooling and next generation sequencing strategy. *J Med Genet* 2011;48:105–16.
- [24] Gajecka M, Mackay KL, Shaffer LG. Monosomy 1p36 deletion syndrome. *Am J Med Genet C* 2007;145C:346–56.
- [25] Wu YQ, Heilstedt HA, Bedell JA, May KM, Starkey DE, McPherson JD, et al. Molecular refinement of the 1p36 deletion syndrome reveals size diversity and a preponderance of maternally derived deletions. *Hum Mol Genet* 1999;8:313–21.
- [26] Colmenares C, Heilstedt HA, Shaffer LG, Schwartz S, Berk M, Murray JC, et al. Loss of the SKI proto-oncogene in individuals affected with 1p36 deletion syndrome is predicted by strain-dependent defects in *Ski*^{-/-} mice. *Nat Genet* 2002;30:106–9.
- [27] Heilstedt HA, Burgess DL, Anderson AE, Chedrawi A, Tharp B, Lee O, et al. Loss of the potassium channel beta-subunit gene, *KCNAB2*, is associated with epilepsy in patients with 1p36 deletion syndrome. *Epilepsia* 2001;42:1103–11.
- [28] Arndt AK, Schafer S, Drenckhahn JD, Sabeh MK, Plovie ER, Caliebe A, et al. Fine mapping of the 1p36 deletion syndrome identifies mutation of *PRDM16* as a cause of cardiomyopathy. *Am J Hum Genet* 2013;93:67–77.
- [29] Potts RC, Zhang P, Wurster AL, Precht P, Mughal MR, Wood III WH, et al. CHD5, a brain-specific paralog of Mi2 chromatin remodeling enzymes, regulates expression of neuronal genes. *PLoS One* 2011;6:e24515.
- [30] Neal J, Apse K, Sahin M, Walsh CA, Sheen VL. Deletion of chromosome 1p36 is associated with periventricular nodular heterotopia. *Am J Med Genet A* 2006;140:1692–5.
- [31] Saito S, Kawamura R, Kosho T, Shimizu T, Aoyama K, Koike K, et al. Bilateral perisylvian polymicrogyria, periventricular nodular heterotopia, and left ventricular noncompaction in a girl with 10.5–11.1 Mb terminal deletion of 1p36. *Am J Med Genet A* 2008;146A:2891–7.
- [32] Descartes M, Mikhail FM, Franklin JC, McGrath TM, Bebin M. Monosomy1p36.3 and trisomy 19p13.3 in a child with periventricular nodular heterotopia. *Pediatr Neurol* 2011;45:274–8.
- [33] Dobyns WB, Mirzaa G, Christian SL, Petras K, Roseberry J, Clark GD, et al. Consistent chromosome abnormalities identify novel polymicrogyria loci in 1p36.3, 2p16.1-p23.1, 4q21.21-q22.1, 6q26-q27, and 21q2. *Am J Med Genet A* 2008;146A:1637–54.
- [34] Thienpont B, Mertens L, Buyse G, Vermeesch JR, Devriendt K. Left-ventricular non-compaction in a patient with monosomy 1p36. *Eur J Med Genet* 2007;50:233–6.
- [35] Cremer K, Ludecke HJ, Ruhr F, Wiczorek D. Left-ventricular non-compaction (LVNC): a clinical feature more often observed in terminal deletion 1p36 than previously expected. *Eur J Med Genet* 2008;51:685–8.
- [36] Gajecka M, Saitta SC, Gentles AJ, Campbell L, Ciprero K, Geiger E, et al. Recurrent interstitial 1p36 deletions: evidence for germline mosaicism and complex rearrangement breakpoints. *Am J Med Genet A* 2010;152A:3074–83.
- [37] Faivre L, Morichon-Delvallez N, Viot G, Martinovic J, Pinson MP, Aubry JP, et al. Prenatal detection of a 1p36 deletion in a fetus with multiple malformations and a review of the literature. *Prenat Diagn* 1999;19:49–53.
- [38] Riegel M, Castellan C, Balmer D, Brecevic L, Schinzel A. Terminal deletion, del(1)(p36.3), detected through screening for terminal deletions in patients with unclassified malformation syndromes. *Am J Med Genet* 1999;82:249–53.
- [39] Redon R, Rio M, Gregory SG, Cooper RA, Fiegler H, Sanlaville D, et al. Tiling path resolution mapping of constitutional 1p36 deletions by array-CGH: contiguous gene deletion or “deletion with positional effect” syndrome? *J Med Genet* 2005;42:166–71.
- [40] Digilio MC, Bernardini L, Lepri F, Giuffrida MG, Guida V, Baban A, et al. Ebstein anomaly: genetic heterogeneity and association with microdeletions 1p36 and 8p23.1. *Am J Med Genet A* 2011;155A:2196–202.
- [41] Sinkovec M, Kozelj M, Podnar T. Familial biventricular myocardial noncompaction associated with Ebstein’s malformation. *Int J Cardiol* 2005;102:297–302.
- [42] Sentex E, Wang X, Liu X, Lukas A, Dhalla NS. Expression of protein kinase C isoforms in cardiac hypertrophy and heart failure due to volume overload. *Can J Physiol Pharmacol* 2006;84:227–38.
- [43] Wu SC, Solaro RJ. Protein kinase C zeta. A novel regulator of both phosphorylation and de-phosphorylation of cardiac sarcomeric proteins. *J Biol Chem* 2007;282:30691–8.
- [44] Kim BJ, Zaveri HP, Shchelochkov OA, Yu Z, Hernandez-Garcia A, Seymour ML, et al. An allelic series of mice reveals a role for RERE in the development of multiple organs affected in chromosome 1p36 deletions. *PLoS One* 2013;8:e57460.
- [45] Barron DJ, Kilby MD, Davies B, Wright JG, Jones TJ, Brawn WJ. Hypoplastic left heart syndrome. *Lancet* 2009;374:551–64.
- [46] Grossfeld PD. The genetics of hypoplastic left heart syndrome. *Cardiol Young* 1999;9:627–32.
- [47] Sanchez-Valle A, Pierpont ME, Potocki L. The severe end of the spectrum: hypoplastic left heart in Potocki–Lupski syndrome. *Am J Med Genet A* 2011;155A:363–6.
- [48] Chen CP, Chern SR, Hsu CY, Lee CC, Lee MS, Wang W. Prenatal diagnosis of de novo partial trisomy 13q (13q22 → qter) and partial monosomy 8p (8p23.3 → pter) associated with holoprosencephaly, premaxillary agenesis, hexadactyly, and a hypoplastic left heart. *Prenat Diagn* 2005;25:334–6.
- [49] Tsuyusaki Y, Yoshihashi H, Furuya N, Adachi M, Osaka H, Yamamoto K, et al. 1p36 deletion syndrome associated with Prader–Willi-like phenotype. *Pediatr Int* 2010;52:547–50.



INVITED REVIEW ARTICLE

Characteristics of 2p15-p16.1 microdeletion syndrome: Review and description of two additional patients

Keiko Shimojima¹, Nobuhiko Okamoto² and Toshiyuki Yamamoto¹¹Institute for Integrated Medical Sciences, Tokyo Women's Medical University, Tokyo, and ²Department of Medical Genetics, Osaka Medical Center and Research Institute for Maternal and Child Health, Izumi, Japan

ABSTRACT Many new microdeletion syndromes have been characterized in the past decade, including 2p15-p16.1 microdeletion syndrome. More than 10 patients with this syndrome have been described. Recently, we encountered two additional patients with 2p15-p16.1 microdeletion syndrome. All patients showed variable degrees of intellectual disability, with the autistic features characteristic of this syndrome. Seven out of 16 patients (44%) showed structural abnormalities in the brain, which is also an important feature of this syndrome. The shortest region of microdeletion overlap among the patients includes two genes, *USP34* and *XPO1*. Although these genes have some functional relevance to cancer, they have not been associated with neurological functions. Diagnosis of additional patients with 2p15-p16.1 microdeletion syndrome and identification of pathogenic mutations in this region will help identify the genes responsible for the neurological features of the syndrome.

Key Words: 2p15-p16.1 microdeletion syndrome, autistic features, intellectual disability, *USP34*, *XPO1*

NEWLY IDENTIFIED RECURRENT MICRODELETIONS

Before the development of chromosomal microarray testing, only a small number of interstitial chromosomal deletions had been clinically recognized, including 22q11.2 deletion syndrome, Williams syndrome, Smith-Magenis syndrome, Sotos syndrome, and Prader-Willi/Angelman syndrome (Emanuel and Shaikh 2001). Because patients with these syndromes show frequently distinct clinical features, clinical examinations can yield an initial diagnosis. The interstitial deletions associated with contiguous gene deletion syndromes are often mediated by surrounding low-copy repeats (LCRs) located on both ends of the deletions (Stankiewicz and Lupski 2002). Therefore, most deletions mediated by LCRs share the same size and the same region. Consequently, patients with such interstitial deletions exhibit common clinical features. After chromosomal microarray testing became widespread, numerous novel interstitial deletions were identified (Nevado et al. 2014), some of which have genomic structures associated with LCRs.

Compared to LCR-mediated microdeletions, microdeletions mediated by random breakpoints are more difficult to diagnose, because the clinical features of the patients carrying random

microdeletions are variable and less distinctive. However, this variability provides an opportunity to study genotype-phenotype correlations and thereby understand the functions of the genes in the deletion region. Williams et al. (2010) analyzed genotype-phenotype correlations in patients with 2q37 deletions and narrowed the critical region for brachydactyly to the histone deacetylase 4 gene (*HDAC4*) region. They then identified *HDAC4* mutations in patients with similar clinical features but no 2q37 deletions, thereby establishing that *HDAC4* is responsible for brachydactyly (Williams et al. 2010). Thus, the study of genotype-phenotype correlations is a powerful way to narrow the list of potential candidate genes.

In 2007, 2p15-p16.1 microdeletion syndrome was reported as an autism-related disorder (Rajcan-Separovic et al. 2007). Patients with 2p15-p16.1 microdeletions have distinctive clinical features associated with variable neurodevelopmental abnormalities. In addition to a patient previously diagnosed by us (Liang et al. 2009), we have identified two additional patients with 2p15-p16.1 microdeletions. Since the publication of the first study, over 10 patients with 2p15-p16.1 microdeletions have been described. However, the genes responsible for the clinical features of the syndrome have not been established. Here, we report on additional patients and review the characteristics of 2p15-p16.1 microdeletion syndrome.

ADDITIONAL NEW PATIENTS

The clinical features of two new patients and previously described patients are summarized in Table 1.

Patient 1

A 3-year-old boy was born at 39 weeks of gestation with a birthweight of 2360 g (3rd–10th centile), a length of 46 cm (3rd–10th centile), and an occipitofrontal circumference (OFC) of 33 cm (25th–50th centile). His parents and elder sister are healthy. Immediately after birth, he exhibited stridor due to laryngomalacia. He had difficulty swallowing. He was able to sit alone at 9 months, walk independently at 21 months, and jump at 3 years. However, he spoke no meaningful words. Brain magnetic resonance imaging (MRI) examined at 12 months revealed corpus callosum agenesis (Fig. 1). He shows irritability and tactile hypersensitivity, suggesting behavior abnormalities. At present, his weight is 13.7 kg (50th–75th centile), his height is 95.9 cm (75th centile), and his OFC is 45 cm (<3rd centile), indicating microcephaly. He has small palpebral fissures, telecanthus, and low-set ears (Fig. 2A).

Patient 2

An 18-year-old female patient was born at 41 weeks of gestation with a birthweight of 2310 g (3rd–10th centile). She has exhibited

Correspondence: Toshiyuki Yamamoto, MD, PhD, Institute for Integrated Medical Sciences, Tokyo Women's Medical University, 8-1 Kawada-cho, Shinjuku-ward, Tokyo 162-8666, Japan. Email: yamamoto.toshiyuki@twmu.ac.jp

Received March 14, 2015; revised and accepted April 14, 2015.

Table 1 Clinical features of patients with microdeletions around 2p15-p16.1

	Rajcan-Separovic et al. 2007		de Leeuw et al. 2008		Chabchoub et al. 2008		Liang et al. 2009		Felix et al. 2010		Prontera et al. 2011		Wohlleber et al. 2011		Huchtagowder et al. 2012		Piccione et al. 2012		Hancarova et al. 2013		Florisson et al. 2013		Fammemel et al. 2014		Jorgez et al. 2014		This study		Total in patients with 2p15-p16.1 microdeletion syndromes§		
	P1	P2									P1	P2			P1	P2			P1	P2	#1	#2	#3	#4	#5	#6	#7	P1		P2	
General																															
Current age (years)	9	7	34	9	4	4	9	8	12	0	2	0.3	11	4	13	21	10	4	11	1	16	14	4	3	18						
Gender	F	M	M	M	F	F	F	M	F	F	F	M	F	M	F	M	M	M	M	M	M	M	M	M	M	M	M	F	M/F = 12/10		
IUGR	+	-	-	NA	+	+	NA	-	-	+	NA	NA	-	NA	NA	-	-	-	-	-	-	-	-	-	-	-	+	+	6/14		
Mild to severe intellectual disability	+	+	+	+	+	+	+	+	+	+	+	+	+	+	+	+	-	+	+	+	+	+	+	+	+	+	+	+	20/20		
Feeding problems	+	+	+	NA	NA	+	+	+	-	+	NA	NA	+	NA	NA	NA	-	-	-	-	+	NA	NA	+	-	+	-	-	9/12		
Short stature	-	+	+	-	+	NA	NA	-	-	+	-	+	+	-	-	-	-	-	+	NA	NA	NA	NA	+	-	+	-	+	8/15		
Microcephaly	+	+	+	-	+	+	+	+	-	+	-	+	+	+	+	-	-	-	+	+	+	NA	NA	+	+	+	+	+	16/19		
Facial features																															
Bitemporal narrowing	+	+	+	NA	-	NA	+	-	-	+	NA	NA	-	+	+	+	NA	NA	NA	NA	NA	+	NA	-	+	-	+	-	10/13		
Receding short forehead	+	+	+	-	-	+	-	-	-	+	NA	NA	-	-	+/-	NA	NA	NA	NA	NA	NA	NA	NA	NA	NA	NA	-	+	6/12		
Strabismus	+	-	+	NA	-	-	-	-	-	+	+	-	+	+	-	-	NA	NA	NA	NA	NA	NA	NA	NA	NA	NA	-	+	7/15		
Ptosis	+	+	+	NA	+	+	+	-	-	-	-	-	+	+	+	+	NA	NA	+	NA	+	NA	+	+	+	+	-	+	13/17		
Telecanthus	+	+	+	+	+	+	+	-	-	+	+	+	+	+	+	+	NA	NA	+	NA	NA	+	NA	+	NA	+	+	+	18/18		
Widened inner canthal distance	+	+	+	NA	+	NA	+	-	-	+	NA	NA	NA	+	+	-	NA	NA	NA	NA	NA	NA	NA	NA	NA	NA	+	-	9/11		
Short palpebral fissures	+	+	+	NA	+	+	+	-	-	-	NA	NA	+	-	-	-	NA	NA	NA	NA	NA	NA	NA	+	+	-	-	7/13			
Down slanting palpebral fissure	+	+	+	+	-	NA	-	-	-	-	+	-	+	-	-	+	NA	NA	+	+	NA	NA	NA	NA	NA	NA	+	+	11/17		
Epicanthal folds	+	+	+	NA	+	NA	+	-	-	+	+	+	+	+	+	-	NA	NA	+	+	NA	NA	NA	NA	NA	NA	+	+	15/16		
Broad/high nasal root	+	+	+	+	+/-	+	+	-	+	+	-	-	+	+	+	+	NA	NA	NA	NA	NA	NA	NA	NA	NA	NA	+	+	13/15		
Prominent nasal tip	+	+	-	+	-	NA	+	-	-	+	NA	NA	+	-	-	+	NA	NA	+	NA	NA	NA	NA	NA	NA	-	+	9/14			

Long, straight eyelashes	+	+	+	NA	-	+	-	-	-	NA	NA	NA	+	-	+	NA	NA	NA	+	NA	NA	NA	NA	-	-	7/12	
Long, thin eyebrows	-	+	-	NA	-	NA	-	-	-	NA	NA	NA	+	-	+	NA	NA	NA	NA	+	NA	NA	NA	-	-	4/11	
Large ears	+	+	-	+	-	+	+	-	-	-	-	-	-	+	-	NA	NA	NA	+	NA	NA	NA	+	-	-	7/16	
Smooth and long philtrum	+	+	+	NA	+	+	+	-	-	NA	+	+	+	+	+	+	NA	+	-	+	13/14						
Smooth upper vermillion border	+	+	+	+	-	NA	+	-	-	NA	-	-	+	-	-	+	NA	+	+	9/14							
Everted lower lip	+	+	+	+	-	NA	+	-	-	+	-	+	+	-	-	-	NA	+	+	10/15							
High narrow palate	+	+	+	+	-	+	+	-	-	+	-	+	+	-	-	NA	NA	NA	+	NA	+	+	NA	-	+	13/18	
Retrognathia	-	+	+	-	+	‡	-	-	-	+	NA	NA	-	-	-	+	NA	NA	‡	NA	NA	NA	NA	+	+	9/15	
Other physical features																											
Widened inter nipple distance	+	+	+	NA	-	+	+	NA	NA	-	NA	NA	+	-	-	-	NA	+	-	7/13							
Extra nipple	-	+	-	NA	-	NA	-	NA	NA	-	NA	NA	-	-	-	+	NA	-	-	2/12							
Camptodactyly	+	+	-	-	-	+	-	NA	NA	NA	-	+	-	+	+	-	NA	NA	+	NA	+	+	+	-	+	10/18	
Metatarsus abductus	+	+	-	-	†	+	-	NA	NA	NA	-	-	+	-	-	NA	-	-	5/14								
Spasticity legs	+	+	-	-	+	NA	+	NA	NA	+	NA	NA	+	-	-	NA	-	-	6/12								
Other																											
Optic nerve hypoplasia	+	+	+	NA	+	-	-	NA	NA	-	-	-	-	-	-	-	NA	-	-	4/15							
Disturbed vision	-	+	+	NA	NA	+	NA	NA	NA	+	NA	NA	+	-	-	NA	NA	NA	+	NA	NA	NA	NA	-	-	6/11	
Hearing loss	-	+	-	NA	-	-	-	NA	NA	-	-	+	-	-	+	+	NA	-	-	4/15							
Frequent upper respiratory infections	+	-	+	NA	-	-	-	NA	NA	+	-	-	-	-	-	NA	NA	NA	NA	+	+	NA	NA	+	-	6/16	
Laryngomalasia	-	+	-	NA	-	NA	-	NA	NA	-	NA	NA	-	-	-	NA	+	-	2/11								
Hydronephrosis	+	+	+	NA	-	-	-	NA	NA	+	-	-	-	-	-	-	NA	NA	NA	NA	-	NA	NA	-	-	4/16	
Hypogonadism	-	+	-	NA	-	-	-	NA	NA	-	+	+	-	-	-	-	+	+	+	+	-	+	+	-	-	6/19	
Attention deficit behavior	+	+	-	-	+	NA	+	NA	NA	NA	+	NA	-	NA	NA	NA	NA	NA	-	NA	+	NA	+	-	-	6/12	
Structure brain abnormalities	+	+	NA	NA	-	-	-	-	-	+	-	+	-	+	NA	-	NA	NA	NA	+	NA	NA	NA	+	-	7/14	

NA, not assessable; †Metatarsus adductovarus rather than Metatarsus abductus; ‡Micrognathia; NA and +/- are not included in the total counts. §The patient reported by Wohlleber *et al.* (2011) and #1, #2, and #7 reported by Jorgez *et al.* (2014), indicated column are shaded, excluded from total counts due to the genotype point of view.

Fig. 1 Brain magnetic resonance imaging (MRI) of patient 1. Parallel dispositions of the lateral ventricles are noted in the T1-weighted axial image (left). Complete loss of the corpus callosum is shown in the T2-weighted sagittal image (right).

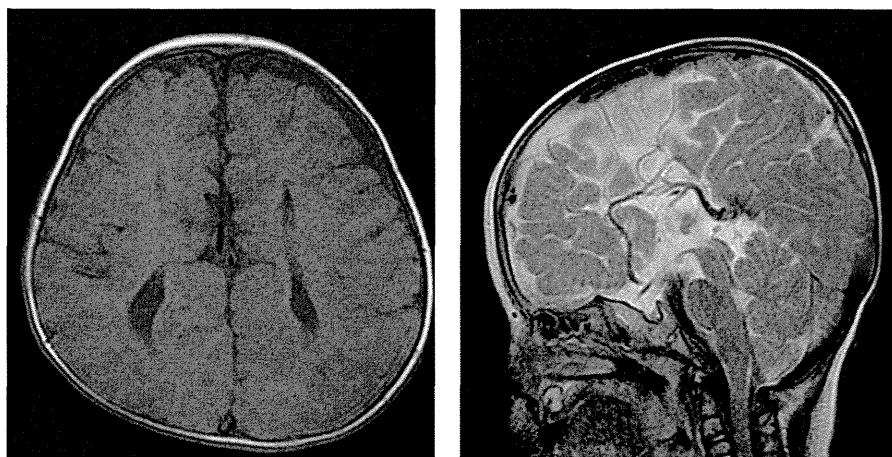
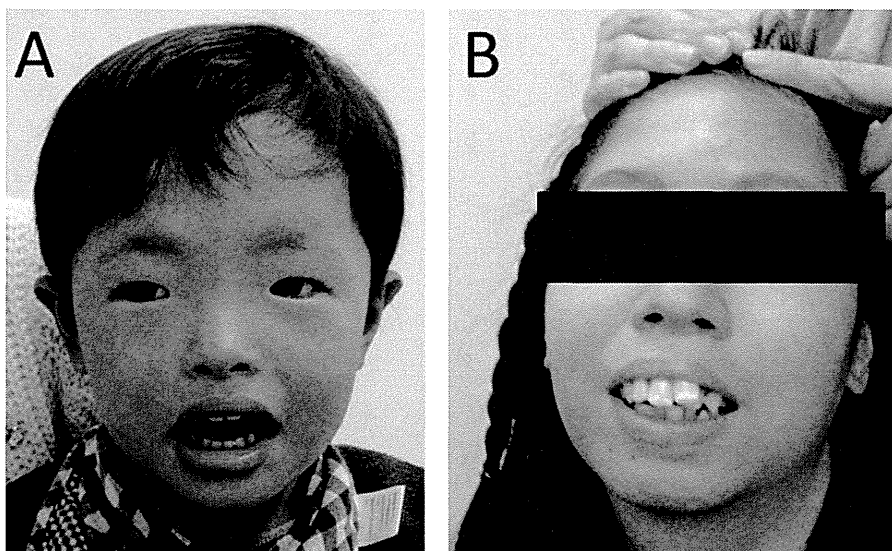


Fig. 2 Distinctive features of the patients. (A) Patient 1 at 3 years has small palpebral fissures, a flat nasal bridge, telecanthus, and low set ears. (B) Patient 2 at 18 years has a small mandible. Written informed consent to use this photograph was obtained from the family of patient 1.



developmental delay since early infancy; she was able to turn over at 9 months and sit at 11 months. She started to walk unsupported at 2 years and 7 months. Brain MRI showed no abnormalities. At present, her weight is 44 kg (3rd–10th centile), her height is 147 cm (<3rd centile), and her OFC is 52.8 cm (<3rd centile), indicating short stature and microcephaly. We also noted the distinctive feature of a small mandible (Fig. 2B). She exhibits severe developmental delay and speaks no meaningful words. Her unbalanced diet and strong resistance to changing her daily life pattern indicate autistic features.

CHROMOSOMAL MICROARRAY TESTING FOR 2P15-P16.1 MICRODELETIONS

This study was performed after receiving approval from the ethics committee at Tokyo Women's Medical University. After obtaining written informed consent from both patients' families, blood samples were obtained from the patients and from the parents of patient 1. Genomic DNA extracted from blood samples was used for further studies. Genomic copy number aberrations were examined using an Agilent Hmn array 60 K (Agilent Technologies, Santa Clara, CA, USA) as described previously (Shimojima et al.

2012). In patient 1, we identified a 238-kb microdeletion in 2p15, indicating $\text{arr } 2\text{p}15(61\ 495\ 220\text{--}61\ 733\ 075) \times 1$. Chromosomal microarray testing using the same platform was performed using DNA from the parents, and the deletion identified in patient 1 was not detected in either parent, indicating a *de novo* origin. Patient 2 had a 3.5-Mb interstitial deletion in 2p14-p15, described as $\text{arr } 2\text{p}15\text{p}14(61\ 618\ 699\text{--}65\ 142\ 743) \times 1$. Because the parents of this patient declined to be genotyped, it is unknown whether the deletion is of *de novo* origin. The presence of the deletions was not confirmed in the described patients (such as by quantitative polymerase chain reaction [PCR]). The deletion regions in both patients are summarized in Table 2 and depicted on the genome map together with those of previously reported patients (Fig. 3). All of the genomic positions refer to build19 in this study.

GENOTYPE-PHENOTYPE CORRELATION

The 2p15-p16.1 microdeletion was first reported in 2007 by Rajcan-Separovic et al. (2007). They described two patients with 2p15-p16.1 microdeletions. The patients shared common features with moderate to severe intellectual disability, autistic features, microcephaly, structural brain anomalies including cortical

Table 2 Deletion regions in patients with 2p15-p16.1 microdeletion syndrome

Researchers	Published year		Deletion region†	
			Start	End
Rajcan-Separovic et al.	2007	P1	56,143,087	61,660,124
		P2	57,307,217	61,660,124
Chabchoub et al.	2007		61,389,240	61,660,124
de Leeuw et al.	2008		57,913,898	61,488,792
Liang et al.	2008		59,241,620	62,385,716
Félix et al.	2010		59,139,200	62,488,871
Prontera et al.	2010		56,853,162	60,380,981
Wohlleber et al.	2011	P1	63,903,236	66,130,003
		P2	62,687,128	65,523,986
Hucthagowder et al.	2012		60,672,255	63,144,695
Piccione et al.	2012	P1	60,604,088	68,391,261
		P2	60,347,280	62,852,277
Hancarova et al.	2013		60,689,977	61,127,979
Florisson et al.	2013	P1	55,661,474	62,509,701
		P2	58,532,874	65,503,931
Fannemel et al.	2014		61,500,346	61,733,075
Jorgez et al.	2014	#1	63,277,168	63,343,150
		#2	62,970,000	68,020,000
		#3	61,130,000	63,520,000
		#4	60,070,000	66,380,000
		#5	61,060,000	65,660,000
		#6	61,570,000	64,320,000
		#7	62,890,000	65,910,000
Present study		P1	61,495,220	61,733,075
		P2	61,618,699	65,142,743

†Genomic positions of chromosome 2 are uniformly translated into build19.

dysplasia/pachygyria, renal anomalies (multicystic kidney, hydronephrosis), digital camptodactyly, visual impairment, strabismus, neuromotor deficits, communication and attention impairments, and a distinctive pattern of craniofacial features. Since the publication of their study, over 10 patients with 2p15-p16.1 microdeletion have been reported that they share similar clinical manifestations (Chabchoub et al. 2008; de Leeuw et al. 2008; Liang et al. 2009; Felix et al. 2010; Prontera et al. 2011; Hucthagowder et al. 2012; Piccione et al. 2012; Florisson et al. 2013; Hancarova et al. 2013; Fannemel et al. 2014). All of the patients were diagnosed with the genotype-first approach using chromosomal microarray testing and all deletions were of *de novo* origin, indicating that copy number losses in this region are pathogenic.

Compared to patients with 2p15-p16.1 microdeletion syndrome, patients whose microdeletions occur closer to the centromeric regions exhibit different clinical features (Fig. 3). Wohlleber et al. (2011) described two patients with microdeletions in 2p14-p15. The deletion regions in the two patients do not overlap with those in the

original cases reported by Rajcan-Separovic et al. (2007) (Fig. 3). Indeed, the patients described by Wohlleber et al. (2011) did not show any distinctive facial features of 2p15-p16.1 microdeletion syndrome. These findings establish a borderline at the 62.5-Mb region, which divides the reported patients into separate categories (Fig. 3). Patients in the first category have deletions closer to the telomeric region, near the chromosome band boundary between 2p16.1 and 2p15. These patients exhibit a typical combination of clinical features, including mild to severe developmental delay, growth delay in association with microcephaly, distinctive features, and brain anomalies.

On the other hand, patients with deletions closer to the centromeric regions, not including the chromosome band boundary between 2p16.1 and 2p15, do not exhibit the characteristics described above. Rather, as Jorgez et al. (2014) have suggested, patients whose chromosomal deletion encompasses the orthodenticle homeobox 1 gene (*OTX1*) region exhibit genitourinary defects with variable penetrance. The study by Jorgez et al. (2014) included seven patients with microdeletions around 2p15; six patients exhibited genitourinary defects. The smallest deletion represented the shortest region of overlap among the patients and included *OTX1*, which might be responsible for the observed genitourinary defects. Although the deletion in patient two reported in this study includes *OTX1*, the patient did not exhibit any genitourinary defects. Moreover, the two patients described by Wohlleber et al. (2011) did not exhibit any genitourinary defects either. Therefore, the phenotypic penetrance of genitourinary defects might be less than 100% in patients with deletions in this region.

Four patients described by Jorgez et al. (2014) had chromosomal deletions that extended to the 2p16.1-2p15 boundary region. Their clinical features were typical of the 2p15-p16.1 microdeletion syndrome, suggesting that the 2p16.1-2p15 boundary region is responsible for the characteristic features (Fig. 3).

In this study, we identified the smallest deletion of 2p15 in patient 1. Upon combining it with the deletion region identified in patient 2, we narrowed the shortest region of the microdeletion overlap to a 114-kb region of chr2:61 618 699-61 733 075. In the overlap region, only two genes are located, the ubiquitin-specific protease 34 gene (*USP34*) and the exportin 1 gene (*XPO1*). Most of the previously identified 2p15-p16.1 microdeletions included this region (Fig. 3). Therefore, *USP34* and *XPO1* are the candidate genes most likely responsible for the characteristic features.

Some patients have deletions that do not include *USP34* and *XPO1*, namely the patients reported by de Leeuw et al. (2008), Hancarova et al. (2013), and Prontera et al. (2011). However, the clinical features of these patients are quite similar to those of the patients whose deletions are restricted to the small regions described above, though they do not overlap. A long-range control of gene expression due to a genomic-positional effect might explain this observation (Kleinjan and van Heyningen 2005).

The original report of 2p15-p16.1 microdeletion syndrome suggested an association with autistic features (Rajcan-Separovic et al. 2007). Many patients with this microdeletion syndrome exhibit autistic features, including the two patients described in the present study. However, most patients exhibit severe intellectual disability, and their autistic features cannot be evaluated with any battery of tests. Patient 1 in this study had the shortest deletion in the 2p15-p16.1 region, but his developmental delay was severe.

BRAIN MALFORMATION

Brain structural abnormalities were observed in 7 of 14 patients (50%) with 2p15-p16.1 microdeletion syndrome (Table 3). Among

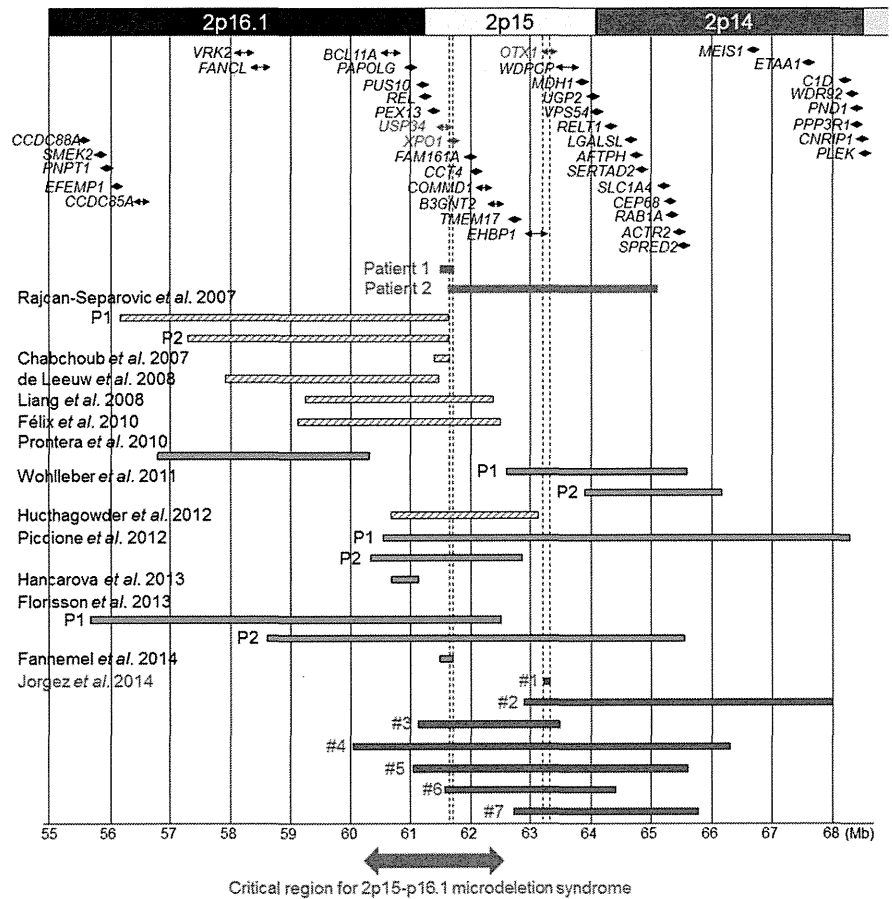


Fig. 3 Genome map of the region around 2p15-p16.1 depicting the aberrations identified in the patients. Bars with arrows on both ends indicate the locations of the genes. Red bars, blue bars, and gray bars indicate the deletion regions identified in the present study, previous studies, and a study by Jorgez et al. (2014), respectively. The shaded gray bars indicate the deletions identified in patients with facial features typical of 2p15-p16.1 microdeletion syndrome. Whereas the parental origins of the deletions in patient 2 in this study and in patients #1 and #2 in the study by Jorgez et al. (2014) were not examined, the de novo origin of all other deletions was confirmed.

Table 3 Brain anomalies in patients with 2p15-p16.1 microdeletion syndrome

Authors		Brain abnormalities
Rajcan-Separovic et al.	P1	Bilateral perisylvian cortical dysplasia
	P2	Dysmyelination Cortical dysplasia Small anterior pituitary and pons
Huchtagowder et al.		Simplified gyral pattern Hypoplasia of the corpus callosum
Piccione et al.	P2	White matter malacia with cerebral atrophy Hypoplastic corpus callosum
Florisson et al.	P1	Simplified gyral pattern Hypoplasia of the corpus callosum Small aspects of the cerebellum and pons
Jorgez et al.	P4	Cerebral atrophy Colpocephaly Enlarged cisterna magna
Present patients	P1	Complete agenesis of the corpus callosum

them, three patients showed hypoplasia of the corpus callosum. Complete agenesis of the corpus callosum was observed for the first time in 2p15-p16.1 microdeletion syndrome in patient 1 of this study (Fig. 1). Thus, brain structural abnormalities, especially those related to the corpus callosum, are characteristic of this syndrome.

GENE FUNCTION

The smallest deletion region in patients with 2p15-p16.1 microdeletion syndrome includes only two genes: *USP34* and *XPO1*.

USP34 is an ubiquitin-specific protease that functions in Wnt signaling and removes ubiquitin modifications from ubiquitinated proteins (Lui et al. 2011). Although this pathway is associated with multiple human diseases, including cancer, the functional relevance of *USP34* haploinsufficiency to the neurological features of 2p15-p16.1 microdeletion syndrome is unknown.

XPO1, also called chromosome region maintenance protein 1 (CRM1), is one of the nuclear transport receptors. Eukaryotic cells are compartmentalized into the cytosol and the nucleus, and communication between the compartments is essential for cell maintenance (Raices and D'Angelo 2012). While seven nuclear export proteins have been identified, *XPO1* uniquely mediates the export of almost all major tumor suppressor proteins (Muqbil et al. 2014). Inhibition of *XPO1* is one approach to restoring the nuclear localization, activation, and function of multiple tumor suppressor proteins. Leptomycin B was the first natural agent identified that irreversibly inhibits *XPO1* (Kau and Silver 2003). However, the